JACS
ARTICLES
Published on Web 01/26/2007

Dimetalloendofullerene $U_2@C_{60}$ Has a U−U Multiple Bond Consisting of Sixfold One-Electron-Two-Center Bonds

Xin Wu and Xin Lu*

Contribution from the State Key Laboratory of Physical Chemistry of Solid Surface and Center for Theoretical Chemistry, Department of Chemistry, College of Chemistry and Chemical Engineering, Xiamen University, Xiamen 361005, China

Received October 16, 2006; E-mail: xinlu@xmu.edu.cn

Abstract: Endohedral metallofullerenes (EMFs) have been extensively studied since their discovery in 1985. Metal−metal bonds, nevertheless, have never been explicitly observed in EMFs synthesized so far. In this contribution, we show by means of all-electron relativistic density functional computations that the dimetalloendofullerene, $U_2@C_{60}$, has an unprecedented U−U multiple bond consisting solely of sixfold ferromagnetically coupled one-electron-two-center bonds with the electronic configuration $(5f\pi_u)^2(5f\sigma_g)^1(5f\delta_g)^2(5f\phi_u)^1$, which are dominated by the uranium 5f atomic orbitals. This bonding scheme is completely distinct from the metal−metal bonds discovered thus far in the d- and f-block polynuclear metal complexes. This finding initiates a connection of the metal−metal multiple bonding chemistry and the fullerene chemistry.

1. Introduction

Endohedral metallofullerenes (EMFs) are fullerene-based derivatives that have a metal atom or a metal-containing cluster inside a hollow fullerene cage.[1] Due to their unique "superatomic" core−shell electronic structures arising from a significant electron transfer from the encapsulated cluster to the fullerene cage, EMFs have attracted wide interests during the past two decades.[1,2] The key factor that governs the stability of EMFs is the number of the electron transfer. The intramolecular electron transfer in EMFs generally results in that the inner cluster and/or the outer fullerene cage preferentially adopt the stable closed-shell electronic configuration (CSEC).[3] This was exemplified by many previous investigations on EMFs, e.g., $Sc_3N@C_n$ ($n = 68, 78, 80$),[4] $Sc_2@C_{66}$,[5] $La_2@C_{72}$,[6] $La_2@C_{80}$,[7] $Ti_2C_2@C_{78}$,[8] and $Sc_2C_2@C_{68}$.[9]

Nowadays, numerous structures of EMFs have been elucidated experimentally and/or theoretically with endohedral cluster varying from one metal atom (e.g., M = La, Y, Sc, Ce in $M@C_{82}$),[1] dimetallic ones (M_2, e.g., M = La, Sc)[5−7] to metal carbide (M_nC_2, M = Sc; $n = 2-4$)[8−10] or trimetallic nitride (M_3N, M = lanthanide or actinide).[4−11] However, no metal−metal bond, to the best of our knowledge, has ever been explicitly observed in EMFs discovered thus far. The concept of metal−metal multiple bonds has profound influence on the polynuclear chemistry and has been in continuous development since its discovery in 1964.[12,13] In general, a metal−metal multiple bond found in a d- or f-block metal complex normally comprises several folds of two-electron-two-center (TETC)

(1) (a) Shinohara, H. *Rep. Prog. Phys.* **2000**, *63*, 843. (b) *Endofullerenes: A New Family of Carbon Cluster*; Akasaka, T., Nagase, S., Eds.; Kluwer Academic Publisher: Dordrecht, The Netherlands, 2002.
(2) Lu, X.; Chen, Z. *Chem. Rev.* **2005**, *105*, 3643.
(3) (a) Fowler, P. W. *J. Phys. Chem. Solids* **1993**, *54*, 1825. (b) Fan, M.-F.; Lin, Z.; Yang, S. *J. Mol. Struct. (THEOCHEM)* **1995**, *337*, 231. (c) Fowler, P. W.; Zerbetto, F. *Chem. Phys. Lett.* **1995**, *243*, 36.
(4) (a) Stevenson, S.; Fowler, P. W.; Heine, T.; Duchamp, J. C.; Rice, G.; Glass, T.; Harish, K.; Hajdu, E.; Bible, R.; Dorn, H. C. *Nature* **2000**, *408*, 427. (b) Olmstead, M. M.; de Bettencourt-Dias, A.; Duchamp, J. C.; Stevenson, S.; Marciu, D.; Dorn, H. C.; Balch, A. L. *Angew. Chem., Int. Ed.* **2001**, *40*, 1223. (c) Stevenson, S.; Rice, G.; Glass, T.; Harich, K.; Croner, F.; Jordan, M. R.; Craft, J.; Hadju, E.; Bible, R.; Olmstead, M. M.; Maitra, K.; Fisher, A. J.; Balch, A. L.; Dorn, H. C. *Nature* **1999**, *401*, 55. (d) Campanera, J. M.; Bo, C.; Poblet, J. M. *Angew. Chem., Int. Ed.* **2005**, *44*, 7230.
(5) (a) Wang, C.-R.; Kai, T.; Tomiyama, T.; Yoshida, T.; Kobayashi, Y.; Nishibori, E.; Takata, M.; Sakata, M.; Shinohara, H. *Nature* **2000**, *408*, 426. (b) Takata, M.; Nishibori, E.; Wang, C. R.; Sakata, M.; Shinohara, H. *Chem. Phys. Lett.* **2003**, *372*, 512. (c) Kobayashi, K.; Nagase, S. *Chem. Phys. Lett.* **2003**, *362*, 373.
(6) (a) Kato, H.; Taninaka, A.; Sugai, T.; Shinohara, H. *J. Am. Chem. Soc.* **2003**, *125*, 7782. (b) Slanina, Z.; Chen, Z.; Schleyer, P. v. R.; Uhlik, F.; Lu, X.; Nagase, S. *J. Phys. Chem. A* **2006**, *110*, 2231.
(7) (a) Shimotani, H.; Ito, T.; Iwasa, Y.; Taninaka, A.; Shinohara, H.; Nishibori, E.; Takata, M.; Sakata, M. *J. Am. Chem. Soc.* **2004**, *126*, 364. (b) Akasaka, T.; Nagase, S.; Kobayashi, K.; Wälchli, M.; Yamamoto, K.; Funasaka, H.; Kako, M.; Hoshino, T.; Erata, T. *Angew. Chem., Int. Ed.* **1997**, *36*, 1643.
(8) (a) Cao, B.; Hasegawa, M.; Okada, K.; Tomiyama, T.; Okazaki, T;. Suenaga, K.; Shinohara, H. *J. Am. Chem. Soc.* **2001**, *123*, 9679. (b) Tan, K.; Lu, X. *Chem. Comm.* **2005**. 4444. (c) Yumura, T.; Sato, Y.; Suenaga, K.; Iijima, S. *J. Phys. Chem. B* **2005**, *109*, 20251. (d) Wu, X.; Lu, X.; Tan, K.; Zhang, Q. E. *J. Nanosci. Nanotech.* **2007**, *7*, in press.
(9) Shi, Z. Q.; Wu, X.; Wang, C. R.; Lu, X.; Shinohara, H. *Angew. Chem., Int. Ed.* **2006**, *45*, 2107.
(10) Iiduka, Y.; Wakahara, T.; Nakahodo, T.; Tsuchiya, T.; Sakuraba, A.; Maeda, Y.; Akasaka, T.; Yoza, K.; Horn, E.; Kato, T.; Liu, M. T. H.; Mizorogi, N.; Kobayashi, K.; Nagase, T. *J. Am. Chem. Soc*. **2005**, *127*, 12500. (b) Tan, K.; Lu, X. *J. Phys. Chem. A* **2006**, *110*, 1176. (c) Tan, K.; Lu, X.; Wang, C. R. *J. Phys. Chem. B.* **2006**, *110*, 11098.
(11) For recent investigations on trimetallic nitride endofullerenes, see: (a) $Tb_3N@C_{84}$: Beavers, C. M.; Zuo, T.; Duchamp, J. C.; Harich, K.; Dorn, H. C.; Olmstead, M. M.; Balch, A. L. *J. Am. Chem. Soc.* **2006**, *128*, 11352. (b) $CeSc_2N@C_{80}$: Wang, X.; Zuo, T.; Olmstead, M. M.; Duchamp, J. C.; Glass, T. E.; Cromer, F.; Balch, A. L.; Dorn, H. C. *J. Am. Chem. Soc.;* **2006**, *128*, 8884. (c) $Lu_3N@C_{80}$: Cai, T.; Xu, L.; Anderson, M. R.; Ge, Z.; Zuo, T.; Wang, X.; Olmstead, M. M.; Balch, A. L.; Gibson, H. W.; Dorn, H. C. *J. Am. Chem. Soc.* **2006**, *128*, 8581. (d) $ScYErN@C_{80}$: Chen, N.; Zhang, E.-Y.; Wang, C.-R. *J. Phys. Chem. B.* **2006**, *110*, 13322.
(12) Cotton, F. A.; Curtis, N. F.; Harris, C. B.; Johnson, B. F. G.; Lippard, S. J.; Mague, J. T.; Robinson, W. R.; Wood, J. S. *Science* **1964**, *145*, 1305.
(13) See, for example: (a) Cotton, F. A. *Acc. Chem. Res.* **1978**, *11*, 225. (b) Trogler, W. C.; Gray, H. B. *Acc. Chem. Res.* **1978**, *11*, 232. (c) Cotton, F. A. In *Reactivity of Metal-Metal Bonds*; Chisholm, M. H., Ed.; American Chemical Society: Washington, D.C., 1981; pp 1−9. (d) Cotton, F. A.; Murillo, L. A.; Walton, R. A. *Multiple Bonds Between Metal Atoms*, 3rd ed.; Springer: Berlin, 2005.

bonds or, in rare cases, is a combination of two-electron-two-center bonds and one-electron-two-center (OETC) bonds. For example, the prototypic $[Re_2Cl_8]^{2-}$ ion has a quadruple Re−Re bond with a ground-state configuration of $(6d\sigma)^2(6d\pi)^4(6d\delta)^2$, i.e., fourfold TETC bonds including one σ-bond, two π-bonds, and one δ-bond.[14] In the recently reported Ar′CrCrAr′ (Ar′ = C_6H_3-2,6(C_6H_3-2,6-$Pr^i{}_2)_2$, Pr^i = isopropyl),[15a] quintuple Cr−Cr bond was disclosed to contain five fold TETC bonds with the electronic configuration of $(3d\sigma)^2(3d\pi)^4(3d\delta)$.[4,15b] Similarly, the f-block metal complex PhUUPh (Ph = phenyl) was recently predicted to have fivefold TETC U−U bonds with predominantly the $(\sigma)^2(\pi)^4(\delta)^4$ state, in which the 7s, 6d, and 5f valence orbitals of U atom are involved in the U−U bonding.[16] More interestingly, Gagliardi and Roos demonstrated by means of high-level *ab initio* calculations that a neutral U_2 molecule has a unique quintuple bond, which is essentially a combination of three TETC bonds ($\sigma^2+2\pi^4$), four OETC bonds ($\sigma^1+\pi^1+2\delta^2$), and two localized 5f electrons.[17] In addition, some other multiply bonded diuranium compounds, e.g., U_2Cl_6, $U_2Cl_8{}^{2-}$, $U_2(OCHO)_4$, $U_2(OCHO)_6$, and $U_2(OCHO)_4Cl_2$, with U−U bond lengths ranging from 2.43 to 2.80 Å, were also predicted to be stable.[18]

The existence of a multiple metal−metal bond was generally accompanied by a shorter bond distance with respect to the singly bonded species.[13] Recent theoretical investigation revealed that caging a neopentane inside the C_{60} (I_h) fullerene can remarkably squeeze a C−C single bond.[19] It is thus interesting to explore whether a multiple M−M bond with a short M−M bond length can be formed when two metal atoms, e.g., U_2, with plenty of valence electrons and orbitals are confined within a C_{60} fullerene. Herein we show by means of all-electron relativistic density functional computations that the dimetalloendofullerene, $U_2@C_{60}$,[20] have a valence state of $[U_2]^{6+}@C_{60}{}^{6-}$ and, more significantly, contains a multiple U−U bond, composed of sixfold OETC bonds corresponding to the electronic configuration of $(5f\pi_u)^2(5f\sigma_g)^1(5f\delta_g)^2(5f\phi_u)^1$.

2. Computational Details

All the density functional theory (DFT) computations of $U_2@C_{60}$ were performed by using the Dmol[3] code[21] with the generalized gradient approximation (GGA) functional of Perdew, Burke, and Ernzerhof (PBE).[22] Other density functionals, such as the revised PBE (RPBE)[23] and the Perdew−Wang 1991 (PW91),[24] were also employed, and they give essentially similar results to the PBE predictions. For closed- and open-shell systems, the spin-restricted and spin-unrestricted algorithms were used, respectively. All-electron double-numerical basis set with polarization functions (DNP) was applied for all atoms. It is known that the relativistic effects play an important role in the chemical and physical properties of molecules containing heavier elements, such as uranium.[25] To take into account relativistic effects, the all-electron scalar relativistic method utilizing the Douglas-Kroll-Hess (DKH) Hamiltonian,[26] which is the most accurate approach available in DMol[3] package, was chosen. The effect of spin−orbit coupling was not considered because this effect, though very critical for free atoms, is generally quenched in large molecules.[27] We should note that more sophisticated description of the bonding pattern in a f-block metal complex such as $U_2@C_{60}$ requires more sophisticated theoretical approaches, which go beyond the single determinant methods and incorporate both electron correlations (the static and dynamic correlations) and relativistic effects (the scalar part and spin−orbit coupling).[25,27] Unfortunately, such sophisticated treatments, which are generally highly resource-demanding and time-consuming, are only applicable to small molecules[17] and unaffordable for such large systems as $U_2@C_{60}$. Nevertheless, the all-electron relativistic density functional computations performed in the present study do cover the electron correlations and the most significant relativistic effects and, at least, are capable of predicting the bonding scheme of $U_2@C_{60}$ qualitatively. Harmonic vibrational analyses were performed by employing the PBE functional with DNP basis sets (denoted as PBE/DNP) for the key stationary points of $U_2@C_{60}$ to determine whether they are real minima or saddle points.

C_{60} has only one fullerenic isomer, i.e., the C_{60} (I_h), that satisfies the well-known isolated-pentagon rule (IPR).[28] In addition to the C_{60} (I_h) isomer, we have also considered some rationally selected non-IPR C_{60} fullerenes for the encapsulation of U_2.

3. Results and Discussion

3.1. The Ground State of $U_2@C_{60}$ (I_h). $U_2@C_{60}$ was first detected by Guo et al. in a Fourier transform-ion cyclotron resonance mass spectroscopic (MS) experiment with an ultrahigh signal intensity relative to other uranium endofullerenes produced by the laser vaporization of a graphite-UO_2 composite disk.[20] Besides $U_2@C_{60}$, MS signals of $U_2@C_{58}$, $U_2@C_{52}$, and $U_2@C_{50}$ were also observed in the experiment, but with lower intensities. This indicated the successive loss of C_2 units, but not the uranium atoms, from $U_2@C_{60}$ molecule. This phenomenon implied that the two uranium atoms were encapsulated inside the C_{60} carbon cage but not externally attached to the cage surface. [20]

Buckminsterfullerene, C_{60} of I_h symmetry, is the smallest IPR-satisfying fullerene and the *only* C_{60} isomer synthesized thus far.[29] Hence, we consider the encapsulation of U_2 into this C_{60} cage first. Figure 1 depicts the optimized structures and symmetries of $U_2@C_{60}$ isomers **1a**−**d** derived from the C_{60} (I_h) fullerene. In isomer **1a**, the U_2 unit is sandwiched between two six-membered rings, resulting in an overall molecular symmetry of D_{3d}. Similarly, in isomers **1b** and **1c**, the U_2 moiety is sandwiched between two C−C bonds (hexagon−hexagon fusions) and two pentagons, respectively. The symmetries of

(14) (a) Cotton, F. A. *Inorg. Chem.* **1965**, *4*, 334. (b) Gagliardi, L.; Roos, B. O. *Inorg. Chem.* **2003**, *42*, 1599.
(15) (a) Nguyen, T.; Sutton, A. D.; Brynda, M.; Fettinger, J. C.; Long, G. J.; Power, P. P. *Science* **2005**, *310*, 844. (b) Brynda, M.; Gagliardi, L.; Widmark, P. O.; Power, P. P.; Roos, B. O. *Angew. Chem., Int. Ed.* **2006**, *45*, 3804.
(16) Macchia, G. L.; Brynda, M.; Gagliardi, L. *Angew. Chem., Int. Ed.* **2006**, *45*, 6210.
(17) (a) Gagliardi, L.; Roos, B. *Nature* **2005**, *433*, 848. (b) Gagliardi, L.; Pyykkö, P.; Roos, B. *Phys. Chem. Chem. Phys.* **2005**, *7*, 2415.
(18) Roos, B.; Gagliardi, L. *Inorg. Chem.* **2006**, *45*, 803.
(19) Huntley, D. R.; Markopoulos, G.; Donovan, P. M.; Scott, L. T.; Hoffmann, R. *Angew. Chem., Int. Ed.* **2005**, *44*, 7549.
(20) Guo, T.; Diener, M. D.; Chai, Y.; Alford, M. J.; Haufler, R. E.; McClure, S. M.; Ohno, T.; Weaver, J. H.; Scuseria, G. E.; Smalley, R. E. *Science* **1992**, *257*, 1661.
(21) (a) Delley, B. *J. Chem. Phys.* **1990**, *92*, 508. (b) Delley, B. *J. Chem. Phys.* **2000**, *113*, 7756. DMol[3] is available as part of Material Studio.
(22) Perdew, J. P.; Burke, K.; Ernzerhof, M. *Phys. Rev. Lett.* **1996**, *77*, 3865.
(23) Hammer, B.; Hansen, L. B.; Norskov, J. K. *Phys. Rev. B* **1999**, *59*, 7413.
(24) Perdew, J. P.; Wang, Y. *Phys. Rev. B* **1992**, *45*, 13244.
(25) For some reviews, see: (a) Powell, R. E. *J. Chem. Educ.* **1968**, *45*, 558. (b) Pitzer, K. S. *Acc. Chem. Res.* **1979**, *12*, 271. (c) Pyykkö, P.; Desclaux, J. P. *Acc. Chem. Res.* **1979**, *12*, 276. (d) Pyykkö, P. *Chem. Rev.* **1988**, *88*, 563.
(26) (a) Douglas, M.; Kroll, N. M. *Acta. Phys.* **1974**, *82*, 89. (b) Koelling, D. D.; Harmon, B. N. *J. Phys. C: Solid State Phys.* **1977**, *10*, 3107.
(27) Roos, B. O.; Malmqvist, P.−A. *Phys. Chem. Chem. Phys.* **2004**, *6*, 2919.
(28) (a) Kroto, H. W. *Nature* **1987**, *329*, 529. (b) Fowler, P.W.; Manoloupoulos, D. E. *An Atlas of Fullerenes*; Oxford University Press: Oxford, 1995.
(29) (a) Kroto, H. W.; Heath, J. R.; O'Brien, S. C.; Curl, R. F.; Smalley, R. E. *Nature* **1985**, *318*, 162. (b) Kadish, K. M., Ruoff, R. S., Eds. *Fullerene: Chemistry, Physical and Technology*; John Wiley & Sons: New York, 2002. (c) Andreoni, W., Ed. *The Physics of Fullerene-Based and Fullerene-Related Materials*; Kluwer: Dordrecht, 2000. (d) Hirsch, A. *Top. Curr. Chem.* **1998**, *199*, 1.

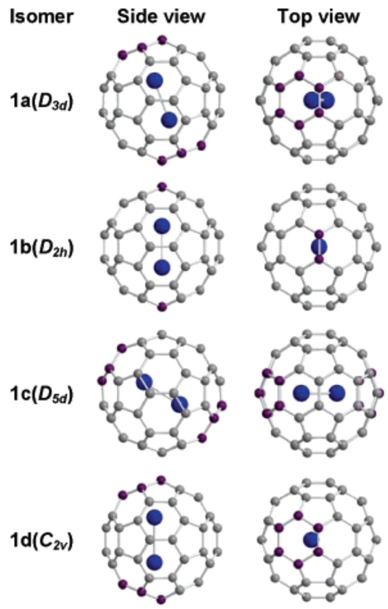

Figure 1. Optimized structures and symmetries of $U_2@C_{60}$ isomers derived from the IPR-satisfying C_{60} (I_h) fullerene. Uranium atoms are represented by large blue balls, the carbon atoms closest to uranium are colored in purple.

1b and **1c** are thus D_{2h} and D_{5d}, respectively. The C_{2v}-symmetric isomer **1d** can be generated from isomer **1a** by moving the U_2 moiety closer to a hemisphere of C_{60}. For each isomer, several electronic states with different spin multiplicities have been computed at the PBE/DNP level of theory. The predicted relative energies and U−U bond lengths are listed in Table 1.

From Table 1, it is clear that the ground-state structure of $U_2@C_{60}$ (I_h) is isomer **1a** in the $^7A_{2u}$ ground state. The predicted U−U bond length in the isomer **1a** ($^7A_{2u}$) is 2.72 Å, much shorter than that in the uranium metal crystal (3.12 Å),[30] suggesting that the U−U bonding in $U_2@C_{60}$ (I_h) is much stronger than that in uranium metal. For isomers **1a** and **1b**, the total energies increase with decreasing spin multiplicities. In sharp contrast, the total energy of isomer **1d** decreases with the decrease of spin multiplicity. For isomer **1c**, its quintet that complies with the Aufbau principle is about 10 kcal/mol more stable than its singlet, triplet, and septet states that do not comfort to the Aufbau principle. In short, the lowest-energy state is $^5A_{1g}$ for isomer **1c**, $^1A_1$ for isomer **1d**, $^7A_{2u}$ for isomer **1a**, and $^7B_{2g}$ for isomer **1b**. That is, the spin state of the molecule depends strongly on the location of the encaged U_2 moiety. In addition, the isomer **1b** ($^7B_{2g}$) and **1d** ($^1A_1$) are about 10 kcal/mol higher than the ground-state structure **1a** ($^7A_{2u}$), suggesting that these structures can be readily approached at room temperature and the $U_2@C_{60}$ (I_h) would display similar intramolecular dynamics as was previously disclosed for $La_2@C_{80}$[7] and $Sc_3N@C_{80}$.[4]

The electronic states of isomer **1a** with different spin multiplicities were further investigated using other density functionals, namely RPBE[23] and PW91.[24] The computed relative energies and U−U bond lengths of these electronic states are listed in Table 2. All three functionals, i.e., PBE, RPBE, and PW91, gave parallel results, showing that the isomer **1a** ($^7A_{2u}$) is the global minimum of $U_2@C_{60}$ derived from the C_{60} (I_h) fullerene. Harmonic vibrational analysis performed at the PBE/DNP level confirmed that the structure **1a** ($^7A_{2u}$) has no imaginary frequency and is a real local minimum on the potential energy surface.

The stability of $U_2@C_{60}$ (**1a**, $^7A_{2u}$) was evaluated in terms of encapsulation energy, which is defined as the exothermicity of the hypothetic reaction,

$$U_2 + C_{60} \rightarrow U_2@C_{60}\ (\mathbf{1a},\ ^7A_{2u})$$

To derive the encapsulation energy, the structures of both U_2 and C_{60} (I_h) were optimized at the PBE/DNP level of theory. However, for U_2, it is in principle impossible to fully reproduce the CASPT2 prediction reported by Gagliardi and Roos[17] under the current framework of density functional theory (DFT), because DFT itself is essentially a single Slater determinant method. Nevertheless, among various spin states of U_2 concerned, the present PBE/DNP calculations predicted a $^7B_{1g}$ ground state with a dissociation energy of ∼35.2 kcal/mol; the U−U bond comprises threefold TETC and fourfold OETC bonds plus two localized 5f electrons (Supporting Information). This DFT prediction agrees reasonably with the CASPT2 prediction that U_2 has a quintuple bond with a dissociation energy of 40.2 kcal/mol,[17] except that the PBE/DNP-predicted U−U bond length (2.52 Å) is about 0.1 Å longer than the CASPT2 value (2.43 Å). The PBE/DNP-computed reaction energy at 0 K (ΔE_r) and enthalpy at 298.15 K ($\Delta H_r^{298.15}$) for the hypothetical encapsulation reaction are −186.7 and −184.8 kcal/mol, respectively.[31] The very large encapsulation energy further verifies the viability of $U_2@C_{60}$ (I_h).

3.2. The Electronic Structure of $U_2@C_{60}$ (I_h) and the Nature of the U−U Multiple Bond. So far we have shown that the ground state of $U_2@C_{60}$ (I_h) is the (**1a**, $^7A_{2u}$) state. In this subsection, we shall introduce its electronic structure as well as the U−U bonding pattern. In general, information of chemical bonding in molecules can be obtained in terms of molecular orbital (MO) analyses.[32] In the DFT-based framework, Kohn−Sham (KS) orbitals are not only associated with the one-electron potential which includes all non-classical effects, but also consistent with the exact ground-state density. The interpretative power of the KS orbitals has been identified by many authors and is therefore recommended as legitimate tools for at least qualitative molecular orbital considerations.[33] Accordingly, a detailed analysis on the KS molecular orbitals of $U_2@C_{60}$ (**1a**, $^7A_{2u}$) has been performed to obtain information about its chemical bonding.

The frontier KS MOs of $U_2@C_{60}$ (**1a**, $^7A_{2u}$) are illustrated in Figure 2. The highest occupied molecular orbital (HOMO), HOMO-1 (doubly degenerate), HOMO-4, and HOMO-5 (doubly degenerate) are singly occupied and dominated by uranium 5f atomic orbitals, whereas the HOMO-2 and HOMO-3 (doubly degenerate) are fully occupied and primarily contributed from the orbitals delocalized over the C_{60} cage. The valence state of $U_2@C_{60}$ (**1a**, $^7A_{2u}$) can be approximately described as $[U_2]^{6+}@C_{60}{}^{6-}$. From Figure 2, the double degenerate HOMO-5 orbitals

(30) The atomic radius of uranium in metallic crystals is 1.56 Å. See Dean, J. A. *Lange's Handbook of Chemistry*, 15th ed.; McGraw-Hill. Inc.: New York, 1999.

(31) $\Delta E_r = E(U_2@C_{60}) - [E(U_2) + E(C_{60})]$; $\Delta H_r^{298.15} = H(U_2@C_{60}) - [H(U_2) + H(C_{60})]$ at 298.15 K.

(32) Hoffman, R. *Acc. Chem. Res.* **1971**, *4*, 1.

(33) See, for example: (a) Kohn, W.; Becke, A. D.; Parr, R. G. *J. Phys. Chem.* **1996**, *100*, 12974. (b) Baerends, E. J.; Gritsenko, O. V. *J. Phys. Chem. A* **1997**, *101*, 5383. (c) Stowasser, R.; Hoffmann, R. *J. Am. Chem. Soc.* **1999**, *121*, 3414. (d) Baerends, E. J. *Theor. Chem. Acc.* **2000**, *103*, 265.

Table 1. PBE/DNP Predicted Electronic States (ES), Relative Energies (ΔE, kcal/mol) and Optimized U−U Bond Lengths (R_{UU}, Å) of IPR-satisfying $U_2@C_{60}$ Isomers (**1a**−**d**)

1a			1b			1c			1d		
ES	ΔE	R_{UU}	ES	ΔE	R_{UU}	ES[a]	ΔE	R_{UU}	ES	ΔE	R_{UU}
$^7A_{2u}$	0.00	2.72	$^7B_{2g}$	9.87	2.66	$^7A_{1g}$*	35.06	2.76	$^7B_2$	10.87	2.74
$^5A_{1g}$	3.97	2.57	$^5B_{1u}$	11.57	2.53	$^5A_{1g}$	26.66	2.49	$^5A_1$	9.83	2.67
$^3A_{1g}$	6.42	2.63	$^3B_{3g}$	12.98	2.50	$^3A_{1g}$*	36.54	2.56	$^3B_1$	5.17	2.54
$^1A_{1g}$	11.93	2.47	^1A_g	13.75	2.47	$^1A_{1g}$*	35.70	2.45	$^1A_1$	6.03	2.42

[a] The electron occupations of the states marked by an asterisk do not comply with the Aufbau principle.

Table 2. Computationally Predicted Electronic States (ES), Relative Energies (ΔE, kcal/mol) and Optimized U−U Bond Lengths (R_{UU}, Å) of $U_2@C_{60}$ (**1a**) by PBE, RPBE, PW91 Density Functionals

	PBE/DNP		RPBE/DNP		PW91/DNP	
ES[a]	ΔE	R_{UU}	ΔE	R_{UU}	ΔE	R_{UU}
$^7A_{2u}$	0.00	2.72	0.00	2.74	0.00	2.72
$^7A_{2g}$	4.55	2.71	4.42	2.73	3.97	2.71
$^5A_{1g}$	3.97	2.57	5.59	2.59	3.42	2.57
$^3A_{1g}$	6.42	2.63	7.62	2.64	3.98	2.63
$^1A_{1g}$	11.93	2.47	14.38	2.49	9.09	2.46
$^7A_{1g}$*	2.46	2.70	2.11	2.72	2.12	2.70
$^7A_{1u}$*	7.76	2.68	7.59	2.69	7.46	2.68
$^3A_{2u}$*	15.11	2.59	16.15	2.59	12.82	2.59
$^9A_{1g}$*	12.43	2.69	11.14	2.71	12.50	2.69

[a] The electron occupations of the states marked by an asterisk do not comply with the Aufbau principle.

Table 3. Estimated U−U Bond Order, U−U Distance (Å), and Bonding Scheme in Some Multiply Bonded Diuranium Compounds

compound	bond order	U–U distance	U–U bonding scheme	ref
U_2	5	2.43	$(\sigma)^2(\pi)^4(\sigma)^1(\delta)^1(\pi)^1(\delta)^1$	17a
U_2^{2+}	3	2.29	$(\sigma)^2(\pi)^4$	17b
PhUUPh	5	2.30	$(\sigma)^2(s)^2(\pi)^4(\delta)^2$	16
$U_2(OCHO)_4$	4	2.33	$(\sigma)^2(\pi)^4(\delta)^2$	18
U_2Cl_6, $U_2Cl_8^{2-}$, $U_2(OCHO)_6$	3	2.40 ∼ 2.44	$(\sigma)^2(\pi)^4$	18
$U_2(OCHO)_4Cl_2$[a]	3	2.80	$(\pi)^4(\delta)^2$	18
$U_2@C_{60}$	3	2.72	$(\pi)^2(\sigma)^1(\delta)^2\ \phi)^1$	this work

[a] The coordination of two axial chloride ions in $U_2(OCHO)_4Cl_2$ results in a U−U triple bond with the structure $(p)^4(d)^2$ and a long U−U distance of 2.80 Å. Its longer U−U distance was explained by the weakness of the δ bond.

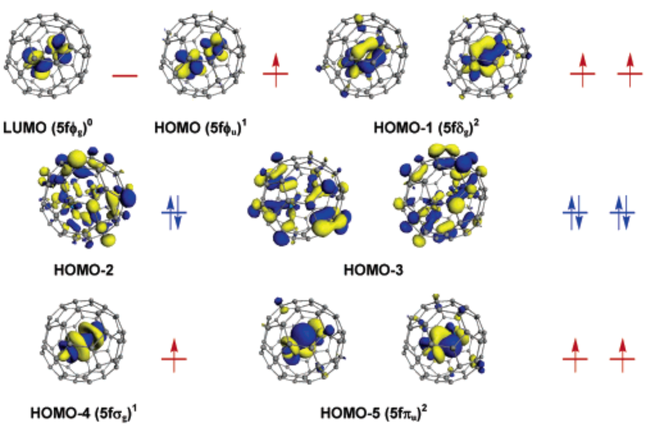

Figure 2. Selected frontier Kohn−Sham orbitals (isodensity value = 0.035) of $U_2@C_{60}$ (**1a**, $^7A_{2u}$).

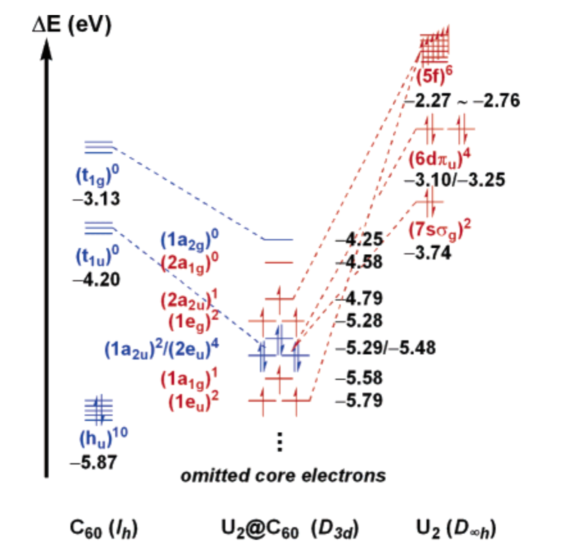

Figure 3. Orbital interaction diagram for $U_2@C_{60}$ (**1a**, $^7A_{2u}$) derived from C_{60} (I_h) and U_2 fragments. Orbital energies (eigenvalues) are given in electron volt (eV). Core electrons are omitted.

correspond to U(5f)−U(5f) π-bonding orbitals; the HOMO-4 is the U(5f)−U(5f) σ-bonding orbital; the two degenerate HOMO-1 orbitals are U(5f)−U(5f) δ-bonding orbitals; the HOMO is U(5f)−U(5f) ϕ-bonding orbital. As such, the electronic configuration of the encapsulated $[U_2]^{6+}$ moiety is $(5f\pi_u)^2(5f\sigma_g)^1(5f\delta_g)^2(5f\phi_u)^1$ and the U−U multiple bond comprises sixfold ferromagnetically coupled one-electron-two-center U(5f)−U(5f) bonds. This extraordinary M−M multiple bond is unprecedented, because normal M−M multiple bond involves merely TETC bonds (e.g., the four TETC bonds in $[Re_2Cl_8]^{2-}$)[14] or a combination of TETC bonds and OETC bonds (e.g., U_2).[17] As summarized in Table 3, it is noteworthy that the U−U bond in $U_2@C_{60}$ (**1a**, $^7A_{2u}$) is much longer than in the quintuply bonded neutral U_2 and PhUUPh,[16,17] the quadruply bonded $U_2(OCHO)_4$, and the triply bonded U_2^{2+} and $U_2(OCHO)_6$, but comparable to the U−U triple bond in $U_2(OCH)_4Cl_2$ (2.80 Å).[18] On the contrary, PBE/DNP-optimization of bare U_2^{6+} ion leads to two unbound U^{3+} cations, evidencing the interaction between two bare U^{3+} cations is strongly repulsive. Therefore, the U−U bond in $U_2@C_{60}$ (**1a**, $^7A_{2u}$) can be empirically recognized as a triple bond and the orbital interactions between the encased U_2 and C_{60} fullerene cage should play an important role on the U−U bond formation.

The nature of the interaction between the U_2 moiety and the C_{60} (I_h) cage can be understood with the help of the orbital interaction diagram depicted in Figure 3. The frontier molecular orbitals of neutral C_{60} (I_h) are highly degenerate. Its HOMO (h_u), LUMO (t_{1u}) and LUMO+1 (t_{1g}) are quintuply, triply, and triply degenerate, respectively. The HOMO (h_u) orbitals are fully occupied with a total of ten electrons. The ground-state electronic configuration of uranium atom is [Rn] $5f^36d^17s$.[2] In a neutral $U_2(^7B_{1g})$ moiety, the U−U TETC bonds are $(7s\sigma_g)^2$-

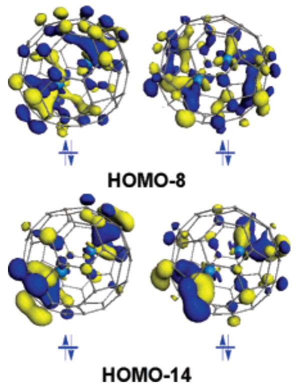

Figure 4. Selected inner Kohn−Sham molecular orbitals (isodensity value = 0.035) of $U_2@C_{60}$ (**1a**, $^7A_{2u}$) with energy much lower than the HOMO region. Both HOMO-8 and HOMO-14 are doubly degenerate with substantial covalent orbital interactions between the C_{60} cage and U atoms.

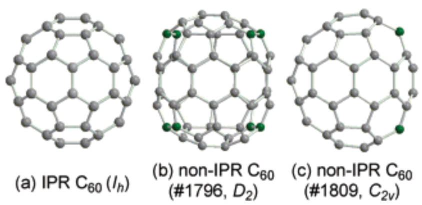

Figure 5. Three selected isomers of C_{60}: (a) IPR-satisfying C_{60} (I_h), (b) non-IPR C_{60} (#1796, D_2), and (c) non-IPR C_{60} (#1809, C_{2v}). The carbon atoms of pentagon−pentagon fusions are colored in green.

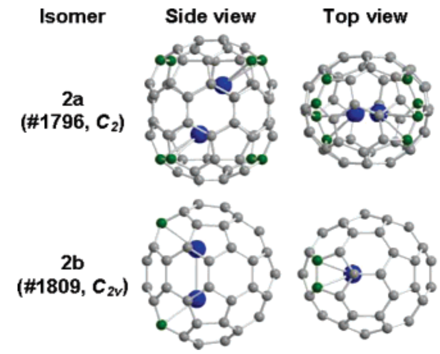

Figure 6. Optimized Geometries of $U_2@C_{60}$ isomers derived from the non-IPR C_{60} (#1796, D_2) and C_{60} (#1809, C_{2v}) cages. The spiral codes of the carbon cages and symmetries of the corresponding non-IPR $U_2@C_{60}$ isomers are given in parentheses. Uranium atoms are represented by large blue balls, the carbon atoms of the pentagon−pentagon fusions are colored in green.

Table 4. PBE/DNP Predicted Electronic States (ES), Relative Energies (ΔE, kcal/mol)[a] and U−U Bond Lengths (R_{UU}, Å) of Non-IPR $U_2@C_{60}$ Isomers **2a** and **2b**

2a			2b		
ES	ΔE	R_{UU}	ES	ΔE	R_{UU}
^1A	21.97	2.67	$^1A_1$	14.83	2.63
^3A	19.20	2.78	$^3B_1$	10.13	2.65
^5A	12.20	3.10	$^5B_1$	10.08	2.66
^7A	10.53	2.99	$^7B_1$	15.44	2.72

[a] Relative to the IPR-satisfying $U_2@C_{60}$ (**1a**, $^7A_{2u}$).

($6d\pi_g$),[4] and the remaining valence electrons are singly distributed with parallel spins on the nearly degenerate molecular orbitals mainly composed of uranium 5f atomic orbitals. Upon formation of $U_2@C_{60}$ (**1a**, $^7A_{2u}$), the six electrons originally occupying the $7s\sigma_g$ and $6d\pi_u$ orbitals of the neutral U_2 fragment are transferred to the empty t_{1u} orbitals of C_{60} (I_h), giving rise to a valence state of $[U_2]^{6+}@C_{60}^{6-}$. Since the whole $U_2@C_{60}$ (**1a**, $^7A_{2u}$) molecule is D_{3d}-symmetric, these three orbitals are no longer degenerate and split into two sets of orbitals, i.e., the $1a_{2u}$ (HOMO-2) and $2e_u$ (HOMO-3). The remaining valence electrons of the U_2 fragment are mainly localized on the U(5f)−U(5f) bonding orbitals with parallel spins, i.e., ferromagnetically coupled, as was discussed in the preceding paragraph. It appears that electron exchange stabilization is dominant here, accounting for such an unusually high-spin ground state.[17]

For a free C_{60}^{6-} (I_h), the HOMO−LUMO gap predicted at the PBE/DNP level is 1.04 eV. For the virtual C_{60}^{6-} anion in $U_2@C_{60}$ (**1a**, $^7A_{2u}$), its “HOMO” and “LUMO” orbitals correspond to the $1a_{2u}$(HOMO−2) and $1a_{2g}$(LUMO+1) MOs of $U_2@C_{60}$ (**1a**, $^7A_{2u}$), respectively (see Figures 2 and 3). At the PBE/DNP level of theory, the “HOMO”−“LUMO” gap of the C_{60}^{6-} anion in $U_2@C_{60}$ (**1a**, $^7A_{2u}$) is 1.04 eV, which is identical to that of a free C_{60}^{6-} anion. Thus, the encapsulation of the $[U_2]^{6+}$ moiety does not change the HOMO−LUMO gap of the C_{60}^{6-} cage, implying ionic (electrostatic) interactions between the encased $[U_2]^{6+}$ and C_{60}^{6-} (I_h). However, a careful examination of the Kohn−Sham MOs of $U_2@C_{60}$ (**1a**, $^7A_{2u}$) with much lower energy than the HOMO region revealed substantial orbital interactions between the C_{60}^{6-} cage and the 5f uranium atomic orbitals with concomitant electron back-donations from the negatively charged carbon cage to the encased metal cations (Figure 4). As a result of such covalent orbital interactions, the closest U−C distances are around 2.48 Å, which is shorter than the U−C distances (avg. 2.93 Å) observed in the U^{3+} compound, $C_6Me_6U(BH_4)_3$.[34a] Hence, the interaction between the encased U_2^{6+} moiety and the C_{60}^{6-} is a mixture of ionic and covalent interactions.

Finally, the chemical stability of $U_2@C_{60}$ (**1a**, $^7A_{2u}$) can be related to the aforementioned electronic structure, i.e., the valence state of $U_2@C_{60}$ (**1a**, $^7A_{2u}$) is $[U_2]^{6+}@C_{60}^{6-}$. Previous experimental and theoretical investigations have revealed that $C_{60}^{6-}(I_h)$ is stable in both solid state and solution since it has a close-shell electronic configuration as well as a large HOMO−LUMO gap.[35] Similar stability could be expected for the $C_{60}^{6-}(I_h)$ anion in $U_2@C_{60}$ (**1a**, $^7A_{2u}$). In addition, the encapsulated uranium atoms in $U_2@C_{60}$ (**1a**, $^7A_{2u}$) are trivalent (+3), which is a formal oxidation state of uranium occurring in many stable compounds.[34]

3.3. $U_2@C_{60}$ Isomers Derived from Non-IPR C_{60} Fullerenes. Though most of the well-characterized EMFs are derived from IPR-satisfying fullerene cages,[1,2] it has been recently shown that a lot of EMFs have non-IPR fullerene cages, e.g., $Ca@C_{72}$,[36] $Sc_3N@C_{68}$,[4] $Sc_2@C_{66}$,[5] $La_2@C_{72}$,[6] $Sc_2C_2@C_{68}$,[9] and $Tb_3N@C_{84}$.[37]

(34) (a) Baudry, D.; Bulot, E.; Charpin, P.; Ephritikhine, M.; Lance, M.; Nierlich, M.; Vigner, J. *J. Organomet. Chem.* **1989**, *371*, 155. (b) Cotton, F. A.; Wilkinson, G. C.; Murillo, A.; Bochmann, M. *Advanced Inorganic Chemistry*, 6th ed.; Wiley-Interscience: New York, 1999.
(35) (a) Tycko, R.; Dabbagh, G.; Rosseinsky, M. J.; Murphy, D. W.; Fleming, R. M.; Ramirez, A. P.; Tully, J. C. *Science* **1991**, *253*, 884. (b) Xie, Q.; Perez-Cordero, E.; Echegoyen, L. *J. Am. Chem. Soc.* **1992**, *114*, 3978. (c) Green, W. H.; Gorun, S. M.; Fitzgerald, G. Fowler, P. W.; Ceulemans, A.; Titeca, B. C. *J. Phys. Chem.* **1996**, *100*, 14892.
(36) (a) Kobayashi, K.; Nagase, S.; Yoshida, M.; Ōsawa, E. *J. Am. Chem. Soc.* **1997**, *119*, 12693−12694. (b) Wan, T. S. M.; Zhang, H. W.; Nakane, T.; Xu, Z. D.; Inakuma, M.; Shinohara, H.; Kobayashi, K.; Nagase, S. *J. Am. Chem. Soc.* **1998**, *120*, 6806. (c) Ichikawa, T.; Kodama, T.; Suzuki, S.; Fujii, R.; Nishikawa, H.; Ikemoto, I.; Kikuchi, K.; Achiba, Y. *Chem. Lett.* **2004**, *33*, 1008.
(37) Beavers, C. M.; Zuo, T.; Duchamp, J. C.; Harich, K.; Dorn, H. C.; Olmstead, M. M.; Balch, A. L. *J. Am. Chem. Soc.* **2006**, *128*, 12352−12353.

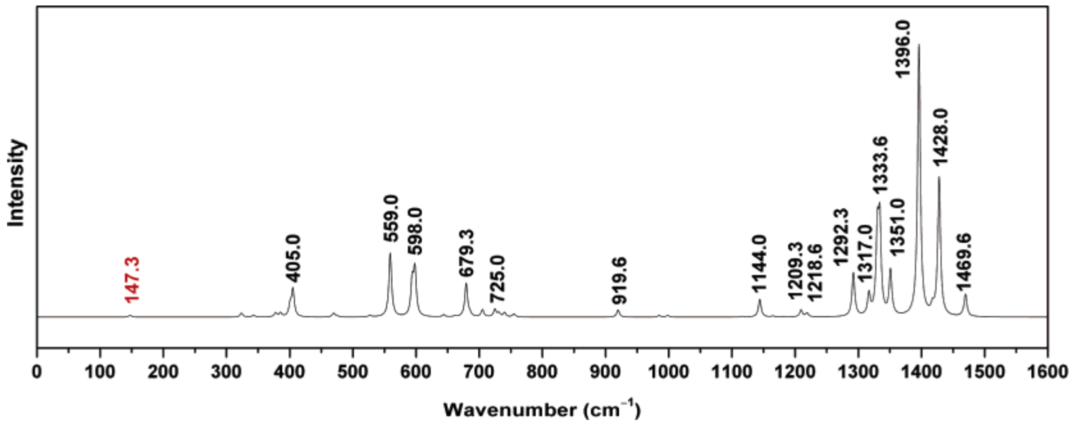

Figure 7. Simulated IR spectrum of $U_2@C_{60}$ (**1a**, $^7A_{2u}$).

Accordingly, in this subsection, we shall consider whether $U_2@C_{60}$ can have more stable isomers with non-IPR carbon cages.

In addition to the IPR-satisfying C_{60} (I_h) isomer, C_{60} has a total of 1811 non-IPR fullerenic isomers according to the spiral algorithm.[28] On account of the electron transfer from the encapsulated U_2 moiety to carbon cage, the relative stability for the hexaanions of all the non-IPR C_{60} isomers (C_{60}^{6-}) have been computed at the semiempirical PM3 level of theory[38] using Gaussian 98 program package[39] (Supporting Information). Among them, the most stable one is the D_2-symmetric #1796 isomer (denoted C_{60}^{6-}(#1796, D_2)) that contains four pentagon−pentagon fusions (PPFs), followed by the C_{2v}-symmetric #1809 isomer (denoted as C_{60}^{6-}(#1809, C_{2v})) that has only two PPFs (Figure 5). At the PM3 level, C_{60}^{6-}(#1796, D_2) and C_{60}^{6-}(#1809, C_{2v}) are 44.8 kcal/mol and 29.7 kcal/mol lower in energy than the IPR-satisfying C_{60}^{6-}(I_h), respectively. Hence, it seems to be possible that $U_2@C_{60}$ isomers derived from these two non-IPR cages would be more stable than the IPR-satisfying $U_2@C_{60}$ (I_h) isomer. To exclude such a possibility, we have computed the total energies of $U_2@C_{60}$ isomers derived from the non-IPR C_{60} (#1796, D_2) and C_{60} (#1809, C_{2v}) and compared them with the IPR-satisfying $U_2@C_{60}$ (I_h).

Figure 6 depicts the optimized geometries of two $U_2@C_{60}$ isomers, **2a** and **2b**, derived from the non-IPR C_{60} (#1796, D_2) and C_{60} (#1809, C_{2v}) cages, respectively. The relative energies of these two isomers with respect to the IPR-satisfying $U_2@C_{60}$ (**1a**, $^7A_{2u}$) are listed in Table 4. The ground state of isomer **2a** is ^7A with an optimal U−U bond length of 2.99 Å, whereas isomer **2b** has a quintet ground state, $^5B_1$, with an optimal U−U bond length of 2.66 Å. It is interesting to note that in both non-IPR $U_2@C_{60}$ isomers the metal atoms are closely attached to the PPFs. Such a phenomenon appears to be prevailing in all EMFs containing non-IPR fullerenes cages, e.g., $Ca@C_{72}$,[36] $Sc_3N@C_{68}$,[4] $Sc_2@C_{66}$,[5] $La_2@C_{72}$,[6] $Sc_2C_2@C_{68}$,[9] and $Tb_3N@C_{84}$.[37]

Similar to the $U_2@C_{60}$ (**1a**, $^7A_{2u}$) case, both **2a**(^7A) and **2b** ($^5B_1$) are found to have the same valence state, $[U_2]^{6+}@C_{60}^{6-}$ or $[U^{3+}]_2@C_{60}^{6-}$. At the PBE/DNP level, isomers **2a**(^7A) and **2b** ($^5B_1$) are by 10.5 and 10.1 kcal/mol less stable than the IPR-satisfying $U_2@C_{60}$ (**1a**, $^7A_{2u}$), respectively. Hence, the IPR-satisfying $U_2@C_{60}$ (**1a**, $^7A_{2u}$) is the global minimum of $U_2@C_{60}$, and the $U_2@C_{60}$ observed in the laser vaporization experiments[20] should have the IPR C_{60} cage, rather than a non-IPR C_{60} cage.

3.4. Vibrational Spectrum of $U_2@C_{60}$ (1a, $^7A_{2u}$). Since $U_2@C_{60}$ (**1a**, $^7A_{2u}$) has six spin-unpaired, ferromagnetically coupling electrons located in the U(5f)−U(5f) bonding orbitals, this molecule should be highly ESR-active, but not detectable in NMR spectroscopic experiment. In addition, Infrared (IR) and Raman spectroscopies have been widely used to characterize metallofullerenes.[1] To assist future experimental characterization, we have computed the vibrational frequencies of this molecule at the PBE/DNP level (Supporting Information). Figure 7 depicts the simulated IR spectrum of this molecule based on the computed vibrational frequencies and IR intensities. Owing to the encapsulation of U_2 unit in C_{60} fullerene cage, the IR spectrum of $U_2@C_{60}$ (**1a**, $^7A_{2u}$) is much more complicated than that of the hollow C_{60} (I_h) fullerene. For the highly symmetric C_{60} (I_h), our PBE/DNP calculation predicted four IR-active vibrational frequencies at 504.6, 574.5, 1197.8 and 1437.0 cm^{-1} (Supporting Information), in agreement with the experimental data (528, 577, 1183, and 1429 cm^{-1}).[40] For $U_2@C_{60}$ (**1a**, $^7A_{2u}$), the encased U_2 moiety in C_{60} (I_h) has two stretching modes, i.e., symmetric and asymmetric modes. In principle, the symmetric U−U stretching mode is IR-inactive, but Raman-active. Hence, this normal mode with a predicted frequency of 168.7 cm^{-1} can be a fingerprint of the U−U bonding in Raman spectroscopic characterization. The asymmetric U−U stretching mode is IR-active with a predicted frequency of 147.4 cm^{-1} and weak IR intensity (1.6 km/mol). The rest of the simulated IR spectrum can be roughly divided into two regions. The peaks ranging from 300 to 750 cm^{-1} arise from bending motions of the carbon cage. The peaks ranging from 920 to 1470 cm^{-1} are due to the C−C stretching modes of the carbon cage. No signals can be observed at frequencies higher than 1500 cm^{-1}.

4. Concluding Remarks

The electronic structures of $U_2@C_{60}$ have been investigated by means of all-electron relativistic density functional computations. The computations revealed the following:

(i) The ground-state structure of $U_2@C_{60}$ has the IPR-satisfying C_{60} (I_h) carbon cage, and the U_2 unit is sandwiched between two six-membered carbon rings in C_{60} (I_h), giving rise to an overall molecular symmetry of D_{3d}.

(38) Stewart, J. J. P. *J. Comput. Chem.* **1989**, *10*, 209.
(39) Frisch, M. J.; et al. *Gaussian 98*, revision A.7; Gaussian, Inc.: Pittsburgh, PA, 1998.
(40) Krätschmer, K.; Lamb, L. D.; Fostiropoulos, K.; Huffman, D. R. *Nature* **1990**, *347*, 354.

(ii) The ground state of $U_2@C_{60}$ (I_h) is $^7A_{2u}$ with a valence state of $[U_2]^{6+}@C_{60}{}^{6-}$ or $[U^{3+}]_2@C_{60}{}^{6-}$. The interaction between the encapsulated $[U_2]^{6+}$ moiety and the $C_{60}{}^{6-}$ cage is not purely ionic but with substantial covalent interaction.

(iii) The encapsulated $[U_2]^{6+}$ moiety has an unprecedented U−U multiple bond comprising sixfold ferromagnetically coupled one-electron-two-center bonds with the electronic configuration of $(5f\pi_u)^2(5f\sigma_g)^1(5f\delta_g)^2(5f\phi_u)^1$.

The significance of the aforementioned finding is two fold. First, it is the first time that a metal−metal bond is found to exist in a metallofullerene. Second, it is the first time to have found a metal−metal multiple bond consisting solely of a set of one-electron-two-center bonds. The present finding settles a conjunction of the polynuclear and fullerene chemistry and, meanwhile, establishes an opening to the forthcoming explorations of the metal−metal interactions and multiple metal−metal bonds in endohedral metallofullerenes.

Acknowledgment. This work was sponsored by NSFC (Grants No. 20425312, 20673088, 20021002, 20203013, 20423002, 90206038), NSF of Fujian Province (Grants No. E0210001 and 2002F010), and Xiamen University through a Minjiang Professorship.

Supporting Information Available: Relative energies of U_2 molecule at different electronic states, frontier KS orbitals of ground-state U_2, the PM3-computed heats of formation and relative energies for the hexaanions of all C_{60} isomers, computed frequencies, and IR intensities of C_{60} (I_h) and $U_2@C_{60}$, the total energies, electronic states and Cartesian coordinates for $U_2@C_{60}$ isomers, and the complete ref 39. This material is available free of charge via the Internet at http://pubs.acs.org.

JA067281G